JOURNAL OF MATERIALS SCIENCE 33 (1998) 2719–2723

Localized superplastic deformation of nanocrystalline 3Y-TZP ceramics under cyclic tensile fatigue at ambient temperature

D. S. YAN, Y. S. ZHENG, L. GAO
The State Key Laboratory of High Performance Ceramics and Superfine Microstructure, Shanghai Institute of Ceramics, Chinese Academy of Sciences, Shanghai, 200050, People's Republic of China

C. F. ZHU, X. W. WANG, C. L. BAI
Institute of Chemistry, Chinese Academy of Sciences, Beijing, 100080, People's Republic of China

L. XU, M. Q. LI
Institute of Nuclear Research, Chinese Academy of Sciences, Shanghai, 201800, People's Republic of China

Cyclic tensile fatigue tests were performed on 100 ± 20 nm, and 0.35 μm 3Y-TZP ceramic specimens at room temperature. Localized superplastic deformation of the grains in the 100 nm material at and near to the fracture surfaces was first identified by AFM imaging. Slip band-like microfeatures, similar to those reported on some metals, were also unexpectedly seen to develop on the side faces. In contrast, the 0.35 μm specimens retained their equiaxed grain morphology after undergoing similar testing conditions. The micromechanisms underlining these phenomena were discussed. Grain boundary diffusion of the respective atomic species is reasoned to be the major governing process in operation. And the contribution of a dislocation slip mechanism is considered to play a possible or parallel role.

1. Introduction

Since the early report of superplasticity in a ceramic material in 1986, a variety of such materials have been shown to exhibit superplastic behaviour at high temperatures [1–8], usually close to their original sintering temperature.

Karch and co-workers [9] in 1987 obtained nanocrystalline CaF_2 (8 nm) which was compacted under high vacuum environment to form a compact by applying a high pressure after collecting the powder in a mould. They showed that the bulk nanocrystalline CaF_2 was plastically deformed at 80 °C to follow the shape of a corrugated iron piston under pressure. Based on the fact that the CaF_2 cubic structure has many slip systems available, Karch *et al.* proposed that the significant plastic deformation occurred by a grain boundary slip (GBS) mechanism, without having examined whether individual grains had been deformed.

Nieh *et al.* [4] reported that the microstructure of the yttrium stabilized tetragonal zirconia polycrystal (Y-TZP) samples superplastically deformed at temperatures higher than 1473 K remained equiaxed, which is consistent to a GBS mechanism.

On the other hand, similar studies on fully stabilized cubic ZrO_2 (C-ZrO_2) single crystals have received considerable attention in recent years [10–14], because the slip planes and directions of C–ZrO_2 are readily identified. These studies were all done at high temperatures.

The objective of this current work was to study the mechanical behaviour of 3Y-TZP ceramic material under cyclic tensile fatigue condition when the grain size is nano-sized, in comparison to the same material having a submicrometre microstructure. This paper will report an unexpected phenomenon that superplastic deformation of the nano-sized grains, at or near to the fatigue crack propagation region, was observed at room temperature. The possible micromechanism underlining this localized superplastic deformation will be discussed.

2. Experimental procedure

2.1. Nano-sized 3Y-TZP powder

The superfine powder was prepared by a coprecipitation method with zirconium oxychloride and yttrium nitrate as the starting materials and NH_4OH solution as the precipitant. The coprecipitated material was washed with deionized water followed with ethanol to remove the unwanted anions as well as to avoid hard

agglomerate formation during calcination. The final powder was obtained by calcining at 750 °C for 2 hr. Characterization was done by Brunauer–Emmett–Teller (BET) method for specific surface area measurement, and by X-ray diffraction (XRD) as well as transmission electron microscopy (TEM) for primary particle size determination. More detailed accounts of nano-sized powder preparation as well as their compaction and densification have been reported elsewhere [15–18]. The average particle size of the powder obtained was 20 nm and no hard agglomerate was present.

2.2. 3Y-TZP bulk specimen preparation

Bulk materials of 3Y-TZP were prepared by hot pressing for 1 h under a pressure of 25 MPa up to a size of $70 \times 70 \times 6$ mm in dimension. The grain size of the bulk materials obtained depended on the maximum temperature chosen; close to full densification was achieved at about 1250 °C and an average grain size of 100 ± 20 nm was identified. When the hot pressing temperature was raised to 1400 and 1550 °C, the average grain size of the material increased to 0.35 μm and 1 μm respectively. Different sized specimens were cut and then ground, polished and bevelled on the edges; they were used to perform the physical and mechanical property measurements. The results are listed in Table I.

2.3. Cyclic fatigue tests

The geometry and dimension of specimens with a 14 mm gauge length for cyclic tensile tests are shown in Fig. 1. Tests were done on a computer-controlled 100 KN Instron servo-hydraulic testing machine Model 8501. An axial extensometer having a gauge length of 10 mm was attached to the central portion of the specimen, allowing a maximum extension of $\pm$ 1 mm. Specimens were cyclically loaded under tension at a load ratio of 0.1 and a frequency of 0.1 Hz (sinusoidal) at ambient temperature. For 100 nm 3Y-TZP specimens, the maximum stress was increased at intervals of 10 MPa up to 60 MPa in steps of 100 cycles at each level. However, for the 0.35 μm specimens, an interval of 50 MPa was used up to 300 MPa also with 100 cycles in between. For both types of tests, most failures occurred at over 500 cycles. All specimens were carefully aligned and all fractures occurred at the gauge section.

TABLE I Basic mechanical properties and microstructural parameters of 3Y-TZP specimens

Hot-pressing temperature (°C/1 h)	Grain size (nm)	Theoretical density (%)	Flexural strength (MPa)	Tensile strength (MPa)
1250	100 ± 20	98.5	480 ± 45	120 ± 20
1400	350	99.2	1250 ± 43	300 ± 25

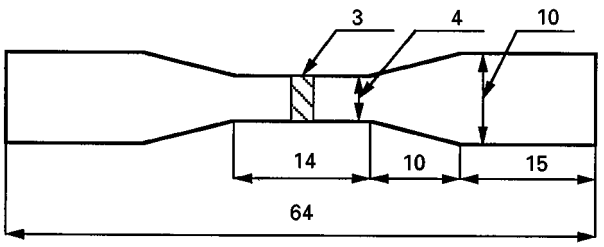

Figure 1 The geometry and dimensions of cyclic tensile test specimen (in millimetres).

2.4. Observation by atomic force microscopy (AFM)

The fracture surfaces were observed by scanning electron microscopy (SEM) and more intensively by AFM as shown schematically in Fig. 2. A Nanoscope-III scanning force microscope (Digital Instruments Inc., USA) was used. The images were obtained in air at ambient temperature. To avoid sample damage, the surface-tip force was minimized by withdrawing the piezo crystal from the scanning stylus while imaging in contact mode. The "Flatten auto" software was used to remove low-frequency noise. All images were recorded in the height mode. Commercial tips provided by Digital Instruments Inc. were used in all these studies. The cantilever length was 200 μm with a spring force constant of 0.12 $N\,m^{-1}$.

3. Results

3.1. Localized superplastic deformation of nanocrystalline specimen

The first indication of some unusually smeared texture at the fractured surfaces of the 100 nm 3Y-TZP specimen was observed by SEM, as shown in Fig. 3. However, the resolution is not good enough to delineate any microstructural features in detail. The next step was to resort to the AFM technique to get clear information close to the atomic level, as described in Section 2.4. Rather unexpectedly, it was found that the nano-sized grains were significantly elongated after cyclic tensile fatigue fracture at room temperature (Fig. 4). The ratio of the long and short axes of the grains were in the range of 4–5 to 8–10. These grains

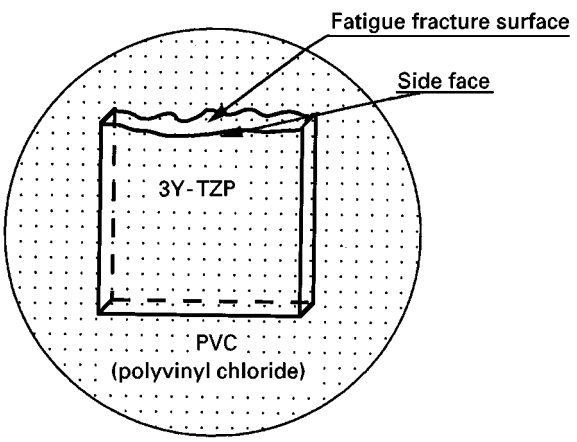

Figure 2 Schematic diagram of the fractured surfaces observed by AFM.

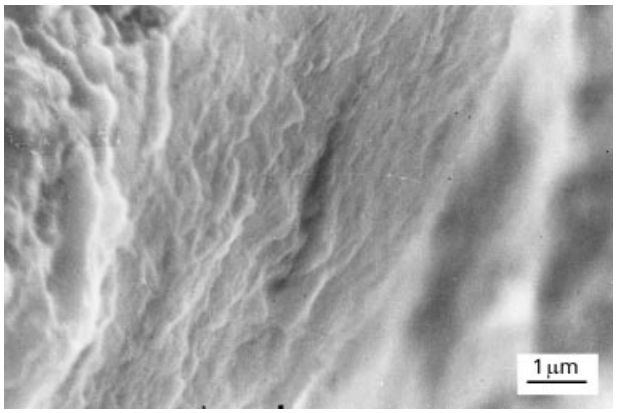

Figure 3 SEM micrograph showing the smeared texture of the fracture surface of nanocrystalline 3Y-TZP ceramics after tensile fatigue.

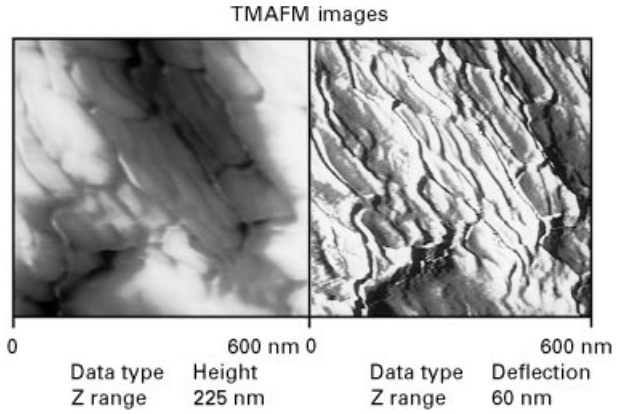

Figure 4 AFM images showing the superplastically deformed 100 nm grain-sized 3Y-TZP specimen after room temperature cyclic fatigue, where the grains were extensively elongated into "banana" shape. Viewed on the fractured surface.

were generally aligned in "banana" shape. For specimens with an average grain size of 0.35 μm, the microstructure of the surfaces after fatigue failure showed equiaxed grains that had retained their original morphology (Fig. 5). The side face of the 100 nm 3Y-TZP specimen from the fractured edge downwards was further studied by AFM imaging. It showed that in a narrow region within a couple of micrometres from each side of the fractured surfaces the morphology of grain elongation appeared to be the general case (see Fig. 6). When the imaging was manipulated to track down a few micrometres on the side surface, it can be seen that the original equiaxed grain morphology remained (Fig. 7), although some slight texture development can also be envisaged (upper left of Fig. 7). It may thus be concluded that localized superplastic deformation of the grains in 100 nm grain size 3Y-TZP specimens had occurred at and near the fracture surfaces, induced by cyclic tensile fatigue.

3.2. Development of slip band-like microfeatures

It was also observed by AFM imaging that microfeatures such as slip bands were developed on the side face of the 100 nm 3Y-TZP specimen after tensile

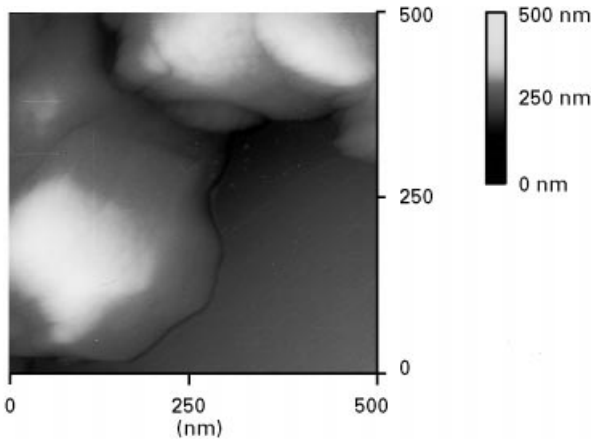

Figure 5 AFM image of 0.35 μm grain-sized 3Y-TZP specimen after room temperature cyclic tensile fatigue. The original grain morphology was retained. (Section viewed on the fracture surface).

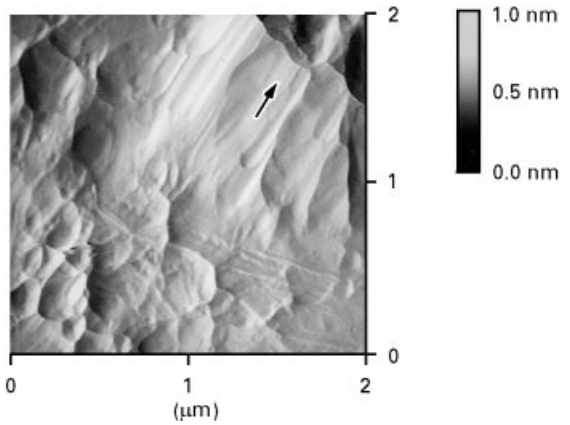

Figure 6 AFM image of 100 nm 3Y-TZP specimen viewed on the side face, after fatigue fracture. An elongated grain morphology was clearly identified close to the fractured surface (upper), while further away, the grains retained essentially the original equiaxed shape (lower left).

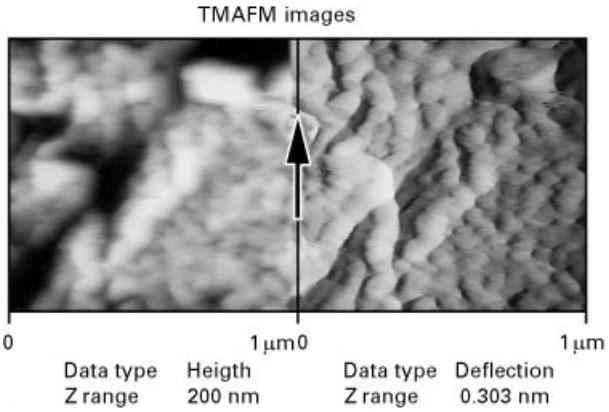

Figure 7 AFM image of 100 nm 3Y-TZP specimen viewed on the side face a few micrometres from the fractured edge. The grains remained their original morphology (lower right), while some slight "texture" development could also be seen (upper left).

fatigue fracture (Fig. 8a). A few 'bumps' were also observed (see arrows in Fig. 8b) on these specimens. This phenomenon had only been reported previously in some metals, especially Cu single crystals [19–24].

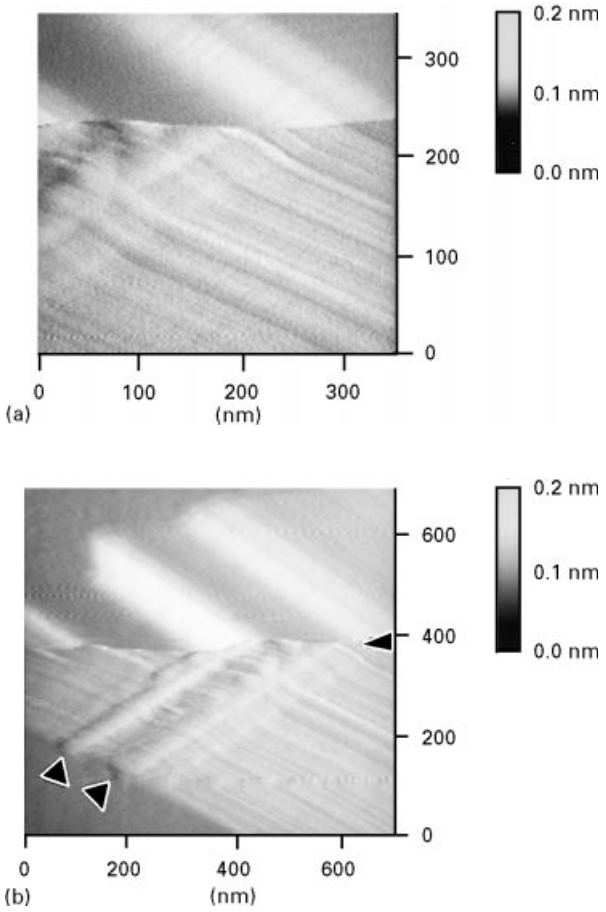

Figure 8 AFM images viewed on the side face of 100 nm 3Y-TZP specimen after fatigue fracture at room temperature. Slip band features are clearly shown (a) and a few 'bumps' (b) can also be seen (arrow).

To the authors' knowledge, this is the first report that an ionic–covalent bonded refractory oxide material exhibited, though in very localized region, superplastic deformation characteristics at room temperature environment, with cyclic tensile fatigue providing the driving force.

4. Discussion

The micromechanism that is responsible for the localized superplastic deformation observed at and near the fractured surfaces of 100 nm grain 3Y-TZP by cyclic tensile fatigue at ambient temperature is the main issue to be discussed. There are two possible mechanisms that could be in operation under the present circumstances, namely, grain-boundary diffusion and dislocation slip. The authors are inclined to believe that the former was the major one to be considered. The arguments are as follows.

4.1. Direct effect of grain size

For grain-boundary diffusion, the rate of deformation, ε, in relation with grain size, d, has been derived by Coble from a simplified model [25], which is represented as

$$\dot{\varepsilon} = B\sigma\Omega\delta D_b/(d^3KT)$$

where σ is the tensile stress, Ω the atomic volume, δ the grain boundary thickness, D_b the grain-boundary diffusivity and KT has the usual meaning. When this equation is used for the present case, σ should be the localized effective tensile stress. The direct effect of fine grain size alone on the rate of deformation can be obtained from the $\dot{\varepsilon} \propto d^{-3}$ relationship. Therefore the 100 nm sized 3Y-TZP material should exhibit some 40 times higher rates of deformation in comparison with the 0.35 μm grain-sized ones, under similar conditions.

4.2. Grain boundary diffusivity in relation with grain size difference

The second point to be argued is that the tetragonal zirconia polycrystal was stabilized by 3 mol % Y_2O_3 with a corresponding amount of oxygen vacancies being generated. This fact should be in favour of promoting ionic diffusion. It is also well known that the yttrium ions tend to segregate at grain boundaries due to the charge and size differences between the Y^{3+} and Zr^{4+} ions. In this respect, 3Y-TZP material with the larger grain size will have grain boundaries possessing lower potential energies caused by this segregation effect. In other words, the submicrometre grain-sized 3Y-TZP material will have more stable grain boundaries, or lower grain-boundary diffusivity than that of the nano-sized material. This can be a factor that has a significant effect on the atomic diffusion along grain boundaries under stress to surpass a threshold that should be existing in either submicrometre-sized grains or 100 nm-sized grains. The experimental evidence given by AFM images showing that the submicrometre grains of the 0.35 μm specimens after cyclic fatigue at room temperature remained equiaxed and those of the 100 nm specimens were extensively elongated (Figs 5 and 4), thus appears to support the above mentioned mechanism. The 100 nm-sized grains offered an environment that is favourable for directional grain boundary diffusion under cyclic fatigue conditions.

If we continue with this analysis, a semi-quantitative estimation of the δD_b values of the 100 nm and the 0.35 μm grain-sized Y-TZP materials can be attempted. For metallic materials, Birringer *et al.* [26] showed that the grain boundary diffusivity of nanocrystalline metal was about three orders of magnitude higher than that in conventional polycrystals. For this material, the deformation or elongation of the nano-sized grains (Fig. 4) can be estimated to be around 400% over a time period of 5000 s. For the submicrometre material in the same time period, the deformation is very small indeed, roughly less than 1%. Using the Coble equation as a basis of comparison, the δD_b value for 100 nm material will be about 10 times larger than that for the 0.35 μm material. In other words, the combined contribution of grain boundary thickness δ and grain boundary diffusion D_b of the 100 nm material on the rate of deformation has been estimated to be around one order of magnitude higher than that of 0.35 μm material. There is also a σ term in this equation. The actual tensile stress used in the fatigue tests was higher for the 0.35 μm grain-sized

specimens as stated above. Therefore, the combined effect of δD_b on the rate of deformation of 100 nm material should still be somewhat higher.

The fact that the 100 nm-sized grains were textured into a "banana" morphology without apparently much change of their relative position seems to offer further support of a grain-boundary diffusion mechanism [27].

The development of a slip-band-like microfeature under cyclic fatigue could also be explained by grain-boundary diffusion mechanism along certain defined directions for the 100 nm 3Y-TZP specimens. When there were two such directions in existence intersecting each other, then the 'bump' formation phenomenon is equally understandable.

4.3. The contribution of dislocation slip

Although the above mentioned arguments are in favour of the grain-boundary diffusion as the controlling mechanism in the development of localized superplastic deformation of the grains in the 100 nm 3Y-TZP material at room temperature under cyclic tensile fatigue, the contribution of a dislocation slip mechanism cannot be completely ruled out. For instance, diffusion motivated dislocation climb and multiplication might be in operation as another or parallel mechanism to develop slip band-like features. However, it is believed that for an ionic–covalent oxide material, it would be of secondary importance. ZrO_2 with Zr^{4+} and O^{2-} would behave considerably differently in comparison with a metal, like Cu and Zn.

5. Conclusion

1. It was first observed by AFM imaging that localized superplastic deformation of nano-sized grains in the 100 nm 3Y-TZP ceramic material at and near to the fracture surfaces was developed after cyclic tensile fatigue at ambient temperature. In comparison, the grains in the 0.35 μm 3Y-TZP ceramics retained their equiaxed morphology under similar cyclic tensile fatigue tests.

2. The micromechanism behind the above mentioned phenomenon is argued to be essentially governed by grain-boundary diffusion. The contribution of dislocation slip might be in operation as a parallel mechanism to develop slip band-like microfeatures.

Acknowledgements

The authors acknowledge the grant by the State Science and Technology Commission under the Climb Project on Nano-material Science. Special thanks are due to Professor Zuyao Xu of Shanghai Jiaotong University and Jianlin Shi of Shanghai Institute of Ceramics for very fruitful and constructive discussions.

References

1. F. WAKAI, S. SAKAGUCHI and Y. MATSUNO, *Adv. Ceram. Mater.* **1** (1986) 259.
2. T. HERMANSSON, K. P. D. LAGERLOF and G. L. DUNLOP, in "Superplasticity and superplastic forming", edited by C. H. Hamilton and N. E. Patont (The Minerals, Metals and Materials Soc., PA, 1988, p. 631.
3. T. G. NIEH, C. M. McNALLY and J. WADSWORTH, *Scripta Metall.* **23** (1989) 457.
4. T. G. NIEH and J. WADSWORTH, *Acta. Metall.* **38** (1990) 1121.
5. I.-W. CHEN and L. A. XUE, *J. Amer. Ceram. Soc.* **73** (1990) 2585.
6. F. WAKAI, Y. KODAMA, S. SAKAGUCHI, N. MURAYAMA, K. IZAKI and K. NIIHARA, *Nature*, **344** (1990) 421.
7. W. J. KIM, J. WOLFENSTINE and D. D. SHERBY, *Acta Metall. Mater.* **39** (1991) 199.
8. J. WITTENANER, T. G. NIEH and J. WADSWORTH, *J. Amer. Ceram. Soc.* **76** (1993) 1665.
9. J. KARCH, R. BIRRINGER and H. GLEITER, *Nature* **330** (1987) 356.
10. D. S. CHEONG, A. DOMINGUEZ-RODRIGUEZ and A. H. HEUER, *Phil. Mag. A* **60** (1989) 123; *ibid.* **63** (1991) 377.
11. E. FRIES, F. GUIBERTEAU, A. DOMINGUEZ-RODRIGUEZ, D. S. CHEONG and A. H. HEUER, *ibid.* **60** (1989) 107.
12. A. DOMINGUEZ-RODRIGUEZ, D. S. CHEONG and A. H. HEUER, *ibid.* **64** (1991) 923.
13. D. HOLMES, A. H. HEUER and P. PIROUZ, *ibid.* **67** (1993) 325.
14. B. YA. FARBER, A. S. CHIARELLI and A. H. HEUER, *ibid.* **70** (1994) 201.
15. J. L. SHI, Z. X. LIN and T. S. YEN (D. S. YAN), *J. Eur. Ceram. Soc.* **8** (1991) 117.
16. J. L. SHI, J. H. GAO, Z. X. LIN and T. S. YEN, *J. Amer. Ceram. Soc.* **74** (1991) 994.
17. J. L. SHI, *J. Eur. Ceram. Soc.* **14** (1994) 505.
18. H. B. QIU, L. GAO, C. D. FENG, J. K. GUO and D. S. YAN, *J. Mater. Sci.* **30** (1995) 5508.
19. J. R. HANCOCK and J. C. GROSSKRETZ, *Acta. Metall.* **17** (1969) 77.
20. A. ABEL, *Mater. Sci. Engng.* **36** (1978) 117.
21. B. T. MA and C. LAIRD, in "Small fatigue cracks", edited by R. O. Ritchie and J. Lankfors (A.I.M.E., 1986) p. 6.
22. A. HUNSCHE and P. NEUMANN, *Acta. Metall.* **34** (1986) 207.
23. K. DIFFERT, U. ESSMANN and H. MUGHRABI, *Phil. Mag. A* **54** (1986) 237.
24. B. T. MA and C. LAIRD, *Acta. Metall.* **37** (1989) 325.
25. R. L. COBLE, *J. Appl. Phys.* **34** (1963) 1679.
26. R. BIRRINGER, U. HERR and H. GLEITER, *Trans. Jpn. Inst. Metall. Suppl.* **27** (1986) 43.
27. T. G. LANGDON, in: Proceedings of the 5th International Conference on "Creep and Fracture Engineering Materials Structures", edited by B. Wilshire and R. W. Evans (Institute of Materials, London, 1993) p. 295.

Received 15 May 1996
and accepted 5 February 1998